PROCEEDINGS OF SCIENCE

Lattice QCD in strong magnetic background

Marco Cardinali,[a] **Massimo D'Elia,**[a] **Lorenzo Maio,**[a,*] **Francesco Sanfilippo**[b] **and Alfredo Stanzione**[c]

[a] *Dipartimento di Fisica dell'Università di Pisa and INFN - Sezione di Pisa, Largo Pontecorvo 3, I-56127, Pisa, Italy*

[b] *INFN - Sezione di Roma Tre, Via della Vasca Navale 84, I-00146, Rome, Italy*

[c] *SISSA, Via Bonomea 265, 34136, Trieste, Italy*

E-mail: marco.cardinali@pi.infn.it, massimo.delia@unipi.it, lorenzo.maio@phd.unipi.it, francesco.sanfilippo@infn.it, alfredo.stanzione@sissa.it

In this work we study the properties of $N_f = 2 + 1$ QCD in the presence of a constant background magnetic field, up to unexplored large values of $|e|B$, by means of lattice Monte Carlo simulations. We investigate the string tension and its asymmetry via the study of the static quark-antiquark potential and of the color flux tube. Moreover, we present preliminary results regarding QCD at finite temperatures in this regime.

The 38th International Symposium on Lattice Field Theory, LATTICE2021 26th-30th July, 2021 Zoom/Gather@Massachusetts Institute of Technology

*Speaker

PoS(LATTICE2021)360

1. Introduction

The study of QCD in a magnetic field provided, along the years, new insights on the strong interacting matter. The discovery of new phenomena of strong interactions in such conditions might be of great phenomenological interest, because it is common to different research fields: from the cosmology of the Primordial Universe, to the non-central ion scattering experiments. Beside that, the effects on the QCD vacuum properties is of undeniable interest also from a purely theoretical point of view: a magnetic field is able to affect the pure gauge sector despite gluons cannot directly interact with it. This could suggest a stronger impact of the magnetic field on the phase structure of the QCD. Recent studies pointed out some interesting properties of the theory in the presence of a very strong external magnetic field. It has been shown that the interactions between a quark antiquark pair are asymmetric in a magnetic background [1–4]. This fact could eventually result in an anisotropic deconfinement when $|e|B \gtrsim 4$ GeV^2 [3]. Moreover it has been shown that, in such conditions, the critical temperature of the chiral restoration drops [5–8], and, for high intensities of the background field, the phase transition is expected to become first order [6, 9].

In this work we explore the properties of the $N_f = 2+1$ QCD, at the physical point for intensities of $|e|B = 4$ GeV^2 and $|e|B = 9$ GeV^2, in order to get direct information about the strong field regime. Fields as strong as these require an accurate tuning of the UV cut-off, which have to be large enough to prevent harmful systematic errors due to discretization. Such a necessity translates into very high computational effort. We performed our measures at both vanishing and finite temperatures, in order to infer information on both the statical potential of a quark-antiquark pair and on the phase diagram. For all measurement we chose a fixed beta prescription, varying, in order to get different magnetic fields and temperature, respectively the number of quanta of magnetic field (see later) and the compact Euclidean time extent. This prescription allowed us to directly perform continuum limits for observables measured at different lattice spacing with identical physical parameters.

The paper is organized as follows: in Section 2 we outline the setup used for the calculations; in Section 3 we present our results at zero and finite temperature; in Section 4 we draw our conclusions.

2. Numerical Methods

We simulated $N_f = 2 + 1$ QCD by means of the tree-level improved Symanzik action in the gauge sector

$$S = -\frac{\beta}{3} \sum_{\mu \neq \nu} \sum_{i} \left(\frac{5}{6} W^{1\times 1}_{i,\mu\nu} - \frac{1}{12} W^{1\times 2}_{i,\mu\nu} \right) \tag{1}$$

where $W^{1\times 1}$ are the plaquettes $W^{1\times 2}$ are the rectangles with area 1×2, and stout improved root staggered fermions in the quark sector

$$D^f_{ij} = a m_f \delta_{i,j} + \sum_{\nu} \frac{\eta_{i;\nu}}{2} \left(U^{(2)}_{i;\nu} \delta_{i,j-\hat{\nu}} - U^{(2)\dagger}_{i-\hat{\nu};\nu} \delta_{i,j+\hat{\nu}} \right) \tag{2}$$

where $U^{(2)}$ are the two times stout smeared gauge links. In Eqs. (1) and (2) the constants β and m_f are the input parameters of the simulation, which have been chosen in order to lay on a line of constant physics, according to the results obtained in [10–12]; a is the lattice spacing and $\eta_{i;\nu}$ are

the staggered phases. The constant background magnetic field B has been inserted along the spatial z-direction, applying the following substitution to the link variables in the fermionic sector

$$U^{(2)}_{j;\mu} \to u^f_{j;\mu} U^{(2)}_{j;\mu}, \tag{3}$$

where $u^f_{i;\mu}$ are $U(1)$ phases defined as follows

$$u^f_{j;y} = e^{ia^2 q_f B j_x}, \quad u^f_{j;x}\big|_{j_x = L_x} = e^{-ia^2 q_f L_x B j_x}, \tag{4}$$

where L_x is the number of lattice points in the x-direction, and all the other $U(1)$ links are set to 1. The right hand side (RHS) of Eq. (4) guarantees the smoothness of the magnetic field across the boundaries [13]. Finally, again because of the periodic boundaries, the magnetic field has to be quantized

$$eB = \frac{6\pi b_z}{a^2 L_x L_y}, \quad b_z \in \mathbb{Z}. \tag{5}$$

To study the confining potential between a static quark-antiquark pair, we used the Wilson loop (W), exploiting the relation [3, 14]

$$aV(a\vec{n}) = \lim_{n_t \to \infty} \log\left(\frac{\langle \mathrm{Tr}\, W(a\vec{n}, an_t)\rangle}{\langle \mathrm{Tr}\, W(a\vec{n}, a(n_t+1))\rangle} \right), \tag{6}$$

where aV is the potential in lattice units and the limit in RHS is practically taken searching for a stable plateau region in the log function for high values of n_t. To determine the microscopic structure of the confining field, we relied on a Wilson loop operator connected to a plaquette probing the longitudinal chromoelectric field

$$\rho^{\mu t}_{\mathrm{conn}}(an_\mu, an_t, x_t) = \frac{3\left\langle \mathrm{Tr}\left(W(an_\mu, an_t) L P^{\mu t}(x_t) L^\dagger\right)\right\rangle - \left\langle \mathrm{Tr}\left(W(an_\mu, an_t)\mathrm{Tr} P^{\mu t}(x_t)\right)\right\rangle}{3\langle \mathrm{Tr}(W)\rangle}, \tag{7}$$

where $P^{\mu t}$ is the plaquette in the μt-plane, L the shortest Shwinger path connecting the plaquette with the Wilson loop at the center of its temporal side, while x_t is the distance between the plaquette and the Wilson loop along one of the directions orthogonal to μ. To get further details on this operator, we refer the reader to [14–16].

To study the chiral symmetry restoration and deconfinement transition, we made use of two fermionic observables, namely the chiral condensate and the quark number susceptibility, defined on the lattice, respectively, as follows

$$\Sigma_f = \frac{T}{V} \frac{\partial \log Z}{\partial m_f}, \tag{8}$$

$$\chi_q = \frac{T}{m_\pi^2 V} \left(\frac{\partial^2 \log Z}{\partial \mu_q^2} \right)_{\mu_q = 0}, \tag{9}$$

where Z is the partition function, μ_q the chemical potential relative to the quark q and m_π is the pion mass. It is worth to note that the observable in Eq. (8) needs for a renormalization to remove additive and multiplicative divergences, thus we used the renormalization defined in [5]

$$\Sigma^r_f = \frac{m_f}{C} \left(\Sigma_f(T, B) - \Sigma_f(0, 0) \right), \tag{10}$$

where C is a normalization constant with the dimensions of a mass to the 4th power. On the other hand, Eq. (9) does not need any renormalization because the quark number susceptibility is connected to a conserved current.

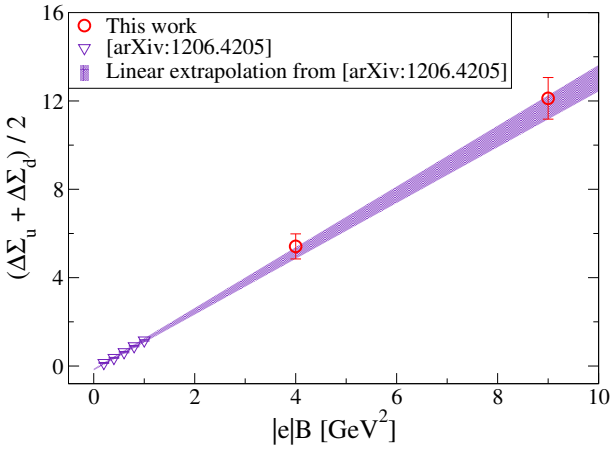

Figure 1: Continuum limits of the chiral condensate in the two simulated background magnetic fields (red circles) compared with data from [17]. The linear extrapolation band put lights on the striking agreement of the new measures with the LLL approximation prediction.

3. Results

Let us start from the magnetic catalysis analysis. In Figure 1 we show the continuum extrapolated chiral condensate measures at vanishing temperature. Here, for the sake of clarity, the results are reported with the renormalization defined in [17] which amounts to set $C = m_\pi^2 F^2$ in Eq. (10), where F^2 is the chiral limit of the pion decay constant. The linear behavior of the chiral condensate for large magnetic fields can be theoretically predicted using the Lowest Landau Level (LLL) approximation: the degeneracy of the LLL linearly increases with $|e|B$, and, because of the Banks–Casher relation, it is proportional to the chiral condensate and hence it is linear in $|e|B$ as well[1]. This result, because of the a^4 dependence of the renormalization group invariant chiral condensate, supports, at the same time, the assumption that the lattice spacing is independent on the magnetic field, an assumption which was directly checked in [5] only for magnetic fields much weaker than those used in this work.

In Figure 2a it is shown the static quark-antiquark potential computed for a lattice spacing 0.0572 fm making use of Eq. (6), which confirms the predictions about the asymmetries caused by the magnetic field [3]: the attractive potential in the longitudinal direction is heavily suppressed, while, on the orthogonal plane, it is slightly enhanced. Such asymmetry is also found in Figure 2b, where we show the values of the string tension σ, obtained through the fit of the Cornell potential

$$V(r) = -\frac{\alpha}{r} + \sigma x + V_0 \tag{11}$$

on the data plotted in Figure 2a. A deconfined theory would exhibit a null string tension, hence the quarks of a pair could be spaced apart up to infinite distance using a finite amount of energy. Such a picture, which seemed possible for magnetic fields stronger than $|e|B \simeq 4$ GeV^2, according to the

[1]This holds for magnetic fields large enough to decouple states with higher energy levels, whose energy is $\propto \sqrt{|e|B}$.

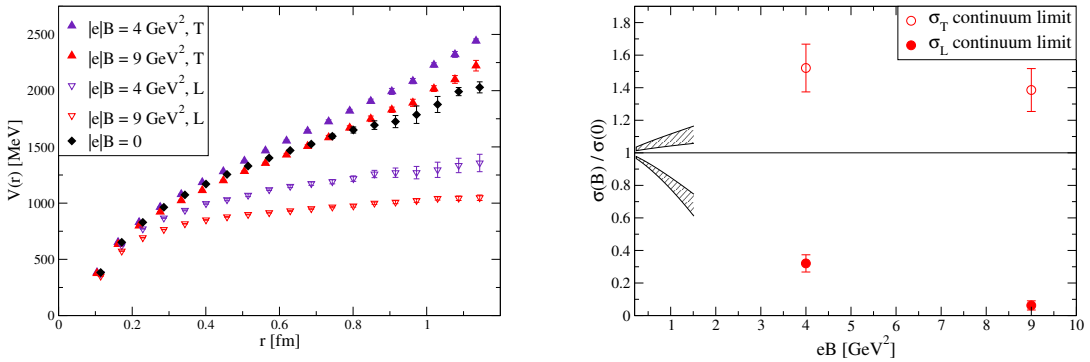

(a) **(b)**

Figure 2: (a) The static potential between a quark-antiquark pair is heavily affected by a strong magnetic field in the longitudinal direction (L), while on the transverse plane it seems to be only moderately enhanced (T). (b) The enhancement effect of the string tension on the plane orthogonal to the magnetic field seems to saturate in the strong magnetic field region explored, while, in the longitudinal direction, it is strongly suppressed, up to an order of magnitude in the 9 GeV^2 case. Nevertheless, the anisotropic deconfinement suggested from the extrapolation performed in [3] is not confirmed by our measures up to, at least, $|e|B = 9$ GeV^2.

extrapolations reported in Ref. [3], is not confirmed, not even for $|e|B = 9$ GeV^2, where the sigma tension is around 2 standard deviations apart from 0.

The same picture of the effects of the magnetic field on the confining potential along the longitudinal direction can be found looking at Figure 3a: it represents the QCD flux tube profile, obtained as

$$E_l(d, x_t) = \frac{1}{a^2 g_0} \rho^{\mu t}_{\text{conn}}(d, x_t), \tag{12}$$

where $\rho^{\mu t}_{\text{conn}}(d, x_t)$ is the lattice observable defined in Eq. (7) with $an_\mu = an_t = d$. The chromoelectric field intensity, computed in the direction longitudinal to the magnetic field, is clearly suppressed. Such an effect is stronger as the magnetic field intensity rises as already pointed out in a weaker field regime [15]. Despite the chromoelectric field is heavily affected from the magnetic field in its intensity, its shape, as function of x_t, appears to be preserved. Relying on this observation, we employed a parameterization based on the form of magnetic fields inside vortices in type II superconductors [18] called Clem ansatz, which well fits numerical results, as shown by the dashed lines in Figure 3a. Clem ansatz allows us to compute the linear energy density,

$$\epsilon(d) = \frac{1}{2} \int d^2 x_t E_l(d, x_t), \tag{13}$$

avoiding the numerical noisy integration. Indeed it is possible to exploit the parameterization in order to compute ϵ as a function of the fit parameters (we refer the reader to [14] and [15] for further details). In Figure 3b we show the continuum extrapolations of the linear density energies for the 4 and 9 GeV^2 magnetic fields compared to the string tensions in the longitudinal direction. We find them compatible within the errors, meaning that the flux tube and the Cornell potential ansatzs are still in good agreement, up to the strongest magnetic field studied. Such a picture is in good

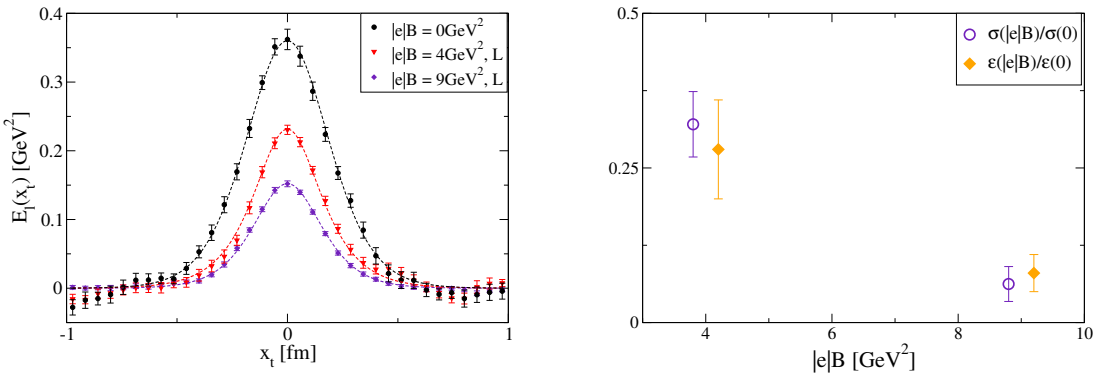

(a) **(b)**

Figure 3: (a) Effects of the magnetic fields on the QCD flux tube in the longitudinal direction. Measures are performed on a $a = 0.0572$ fm lattice, with a quark-antiquark separation $d = 0.68$ fm. The confining chromoelectric field profile is suppressed by the presence of the magnetic field. Despite that, the Clem ansatz is still a good fitting approximation. (b) Clem ansatz is confirmed as a good model for the chromoelectric confining field even at magnetic fields as strong as $|e|B = 9$ GeV^2: the linear energy density computed using this approximation is compatible with the string tension within errors.

agreement with the claim that the magnetic field does not cause anisotropic deconfinement up to $|e|B = 9$ GeV^2 intensities.

We now turn to a brief description of our finite T results. To perform simulations at different temperatures, as anticipated, we used a fixed scale prescription, varying the compact Euclidean time extent L_t of the lattice in order to simulate different temperatures according to the relation

$$T = \frac{1}{aL_t}, \quad \text{with} \quad k_B = 1. \tag{14}$$

To extract the transition temperature, we measured, for every simulated temperature, the quark number susceptibility and the chiral condensate, defined, respectively, in Eqs. (9) and (10), setting, in the latter, $C = m_\pi^4$. In Figure 4a we report the measures at the finest lattice spacing. The transition temperature is taken as the abscissa of the inflection points of the profiles in temperature, which are obtained fitting a suitable function on the numerical data. The shaded region in Figure 4a is the resulting estimate of the transition temperature. The systematic error is evaluated comparing the result for T_c using different fitting functions. In Figure 4b we compare our continuum extrapolated transition temperatures with the large $|e|B$ extrapolation performed in [6]: with respect to that prediction we find a deconfinement transition temperature slightly lower but nevertheless compatible within the errors.

The accordance between transition temperatures computed via the chiral condensate and the quark number susceptibility is a signal that the transition is moving toward a real phase transition, a natural extension of our study is then to deduce the transition nature. A first order transition is characterized by a discontinuous change in the order parameters as the temperature crosses its critical value. This is not to the situation pictured in Figure 4a, which shows a smooth change of the order parameters across the transition, even if the probed temperature are discretely spaced at

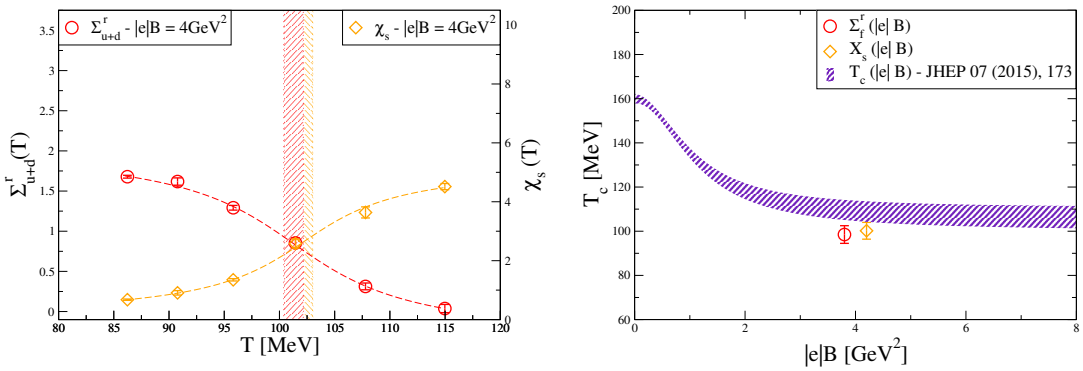

(a) **(b)**

Figure 4: (a) The critical temperatures are obtained for different order parameters by means of a fitting procedure on their temperature profile with an inflecting curve. These values happens to coincide within the errors. (b) Continuum extrapolated critical temperatures for both chiral condensate and baryon quark number susceptibility, compared with extrapolation from [6]: our results are comparable within errors.

intermediate temperatures. A more comprehensive study about these aspects has been reported recently in Ref [19], where results at $|e|B = 9$ GeV^2 are included, showing that indeed the transition is first order in that case.

4. Conclusions

To resume, we explored the QCD properties in the presence of two strong background magnetic fields, namely: $|e|B = 4$ and 9 GeV^2 at both vanishing and finite temperature. For what concerns the former case, we found the expected significant influence of the magnetic background on the confinement properties, but the picture of an anisotropic deconfinement is not confirmed even for magnetic fields up to $|e|B = 9$ GeV^2 [14]. In the finite temperature regime our measurements confirm the influence of the external field on the phase diagram as a lowering in the critical temperature which is of the same entity as that predicted in [6] for the $|e|B = 4$ GeV^2 background. For complete results in this regime we refer the reader to [19], where a deep exploratory study of the magnetic field effect on the QCD phase diagram has been reported.

Acknowledgments

Numerical simulations have been performed on the MARCONI and MARCONI100 machines at CINECA, based on the Projects IscrB_STROMAG IscrB_QGPSMF and on the agreement between INFN and CINECA (under projects INF20_npqcd, INF21_npqcd). F.S. is supported by the Italian Ministry of University and Research (MUR) under grant PRIN20172LNEEZ and by INFN under GRANT73/CALAT.

References

[1] C. Bonati, M. D'Elia, M. Mariti, M. Mesiti, F. Negro and F. Sanfilippo, *Anisotropy of the quark-antiquark potential in a magnetic field*, *Phys. Rev. D* **89** (2014) 114502 [1403.6094].

[2] C. Bonati, M. D'Elia and A. Rucci, *Heavy quarkonia in strong magnetic fields*, *Phys. Rev. D* **92** (2015) 054014 [1506.07890].

[3] C. Bonati, M. D'Elia, M. Mariti, M. Mesiti, F. Negro, A. Rucci et al., *Magnetic field effects on the static quark potential at zero and finite temperature*, *Phys. Rev. D* **94** (2016) 094007.

[4] C. Bonati, M. D'Elia, M. Mariti, M. Mesiti, F. Negro, A. Rucci et al., *Screening masses in strong external magnetic fields*, *Phys. Rev. D* **95** (2017) 074515 [1703.00842].

[5] G. S. Bali, F. Bruckmann, G. Endrodi, Z. Fodor, S. D. Katz, S. Krieg et al., *The QCD phase diagram for external magnetic fields*, *JHEP* **02** (2012) 044 [1111.4956].

[6] G. Endrodi, *Critical point in the QCD phase diagram for extremely strong background magnetic fields*, *JHEP* **07** (2015) 173 [1504.08280].

[7] M. D'Elia, F. Manigrasso, F. Negro and F. Sanfilippo, *QCD phase diagram in a magnetic background for different values of the pion mass*, *Phys. Rev. D* **98** (2018) 054509 [1808.07008].

[8] G. Endrodi, M. Giordano, S. D. Katz, T. G. Kovács and F. Pittler, *Magnetic catalysis and inverse catalysis for heavy pions*, *JHEP* **07** (2019) 007 [1904.10296].

[9] H.-T. Ding, C. Schmidt, A. Tomiya and X.-D. Wang, *Chiral phase structure of three flavor QCD in a background magnetic field*, *Phys. Rev. D* **102** (2020) 054505 [2006.13422].

[10] Y. Aoki, S. Borsanyi, S. Durr, Z. Fodor, S. D. Katz, S. Krieg et al., *The QCD transition temperature: results with physical masses in the continuum limit II.*, *JHEP* **06** (2009) 088 [0903.4155].

[11] S. Borsanyi, G. Endrodi, Z. Fodor, A. Jakovac, S. D. Katz, S. Krieg et al., *The QCD equation of state with dynamical quarks*, *JHEP* **11** (2010) 077 [1007.2580].

[12] S. Borsanyi, Z. Fodor, C. Hoelbling, S. D. Katz, S. Krieg and K. K. Szabo, *Full result for the QCD equation of state with 2+1 flavors*, *Phys. Lett. B* **730** (2014) 99 [1309.5258].

[13] M. H. Al-Hashimi and U. J. Wiese, *Discrete Accidental Symmetry for a Particle in a Constant Magnetic Field on a Torus*, *Annals Phys.* **324** (2009) 343 [0807.0630].

[14] M. D'Elia, L. Maio, F. Sanfilippo and A. Stanzione, *Confining and chiral properties of QCD in extremely strong magnetic fields*, 2109.07456.

[15] C. Bonati, S. Calì, M. D'Elia, M. Mesiti, F. Negro, A. Rucci et al., *Effects of a strong magnetic field on the QCD flux tube*, *Phys. Rev. D* **98** (2018) 054501 [1807.01673].

[16] P. Cea, L. Cosmai, F. Cuteri and A. Papa, *Flux tubes in the QCD vacuum*, *Phys. Rev. D* **95** (2017) 114511 [1702.06437].

[17] G. S. Bali, F. Bruckmann, G. Endrodi, Z. Fodor, S. D. Katz and A. Schafer, *QCD quark condensate in external magnetic fields*, *Phys. Rev. D* **86** (2012) 071502 [1206.4205].

[18] J. R. Clem, *Simple model for the vortex core in a type II superconductor*, *Journal of Low Temperature Physics* **18** (1975) 427.

[19] M. D'Elia, L. Maio, F. Sanfilippo and A. Stanzione, *Phase diagram of QCD in a magnetic background*, 2111.11237.